First bryozoan fauna from the Eocene–Oligocene transition in Tanzania

Emanuela Di Martino[a*], Paul D. Taylor[a], Laura J. Cotton[b, c] and Paul N. Pearson[d]

[a]*Department of Earth Sciences, Natural History Museum, Cromwell Road, London SW7 5BD, UK;* [b]*Naturalis Biodiversity Centre, Darwinweg 2, PO Box 9517, 2300 RA Leiden, The Netherlands;* [c] *School of Biological Sciences, The University of Hong Kong, Kadoorie Biological Sciences Building, Pokfulam Road, Hong Kong SAR, China;* [d]School *of Earth and Ocean Sciences, Cardiff University, Main Building, Park Place, Cardiff CF10 3AT, UK*

Records of Cenozoic tropical bryozoan faunas are sparse, particularly from Africa. Here we describe a previously unknown bryozoan 'sand fauna' from a drill core across the Eocene–Oligocene boundary from a hemipelagic clay succession in Tanzania. Although low in diversity, this well-preserved fauna includes four cheilostome species, all new to science: *Heteractis tanzaniensis* sp. nov., *Bragella pseudofedora* gen. et sp. nov., *Lacrimula kilwaensis* sp. nov. and *L. crassa* sp. nov. The four species vary in mineralogy, with *H. tanzaniensis* having an entirely aragonitic skeleton, *B. pseudofedora* being bimineralic and the two species of *Lacrimula* calcitic. These species have either free-living 'lunulitiform' (*H. tanzaniensis*) or rooted 'conescharelliniform' (*B. pseudofedora*, *L. kilwaensis* and *L. crassa*) colonies adapted to life on a soft, unstable seafloor. The peak occurrence of bryozoans in the core coincides with the Eocene–Oligocene Glacial Maximum (EOGM), characterized by global environmental change from a greenhouse to an icehouse world, sea-level fall, cooling

of the oceans and changes in water circulation that may have led to enhanced nutrient levels favourable to bryozoans both in Tanzania and elsewhere.

*Corresponding author Email: e.di-martino@nhm.ac.uk

Introduction

Compared with higher palaeolatitudes, the Cenozoic tropics have a poor fossil record of bryozoans. This is due to a number of factors including lack of collection effort, deep weathering of outcrops with dense coverage of vegetation, diagenetic loss of aragonitic species and strong lithification making it difficult to observe small encrusting species that dominate tropical bryozoan faunas (Taylor & Di Martino 2014). Published records of Cenozoic fossil bryozoans from tropical East Africa are limited to the papers of Thomas (1961) and Keij (1973) on the enigmatic genus *Skylonia* from the Miocene of Kenya. There is a similar paucity of information on modern East African bryozoan faunas. The bryozoan fauna from Mauritius was first described by Kirkpatrick (1888) and revised a century later by Hayward (1988), the Kirkpatrick paper identifying 34 cheilostomes and three cyclostomes, while >100 cheilostome species were described in Hayward's work. Gurgel & Vasseur (1974) recorded 28 species from the Mozambique Channel and Battistini *et al.* (1976) listed 95 species from the same area. Following the early studies of bryozoans from Zanzibar by Waters (1913, 1914), Cook (1966) and Brood (1976) described seven cheilostomes and 34

3

cyclostomes, respectively. Specifically, the bryozoan fauna described by Cook (1966) led to the introduction of the term 'sand fauna' to refer to those morphotypes capable of directly colonizing fine-grained particulate sediments, unlike most bryozoans for which the availability of large, firm substrata is usually a requirement for the settlement of the larvae and development of the colonies. Some specialized families – including, among others, Lunulitidae, Cupuladriidae, Setosellinidae, Mamilloporidae, Conescharellinidae, Orbituliporidae and Batoporidae – have evolved the ability to colonize the small, unstable substrates typical of muddy or sandy seafloors, from shallow- to deep-water environments. All of these families are cheilostomes with free-living or rooted colonies, morphotypes that first appeared during the Late Cretaceous (McKinney & Jackson 1989).

The principal objective of the present paper is to describe a previously unknown bryozoan 'sand fauna' from a drill core across the Eocene–Oligocene boundary (EOB) from a hemipelagic clay succession in Tanzania. Previous studies of this drill core have examined in detail the turnover pattern in planktonic foraminifera (Wade & Pearson 2008; Pearson & Wade 2015), calcareous nannofossils (Dunkley Jones *et al.* 2008a, b), benthic foraminifera (Cotton & Pearson 2011) and micro-gastropods (Cotton *et al.* in prep.). Here we assess the record of bryozoans. It is emphasized that the Tanzanian succession has an imprint of both global environmental change, as seen for example in the oxygen isotope stratigraphy (Pearson *et al.* 2007), and local effects related to the profound sea level changes that occurred during the Eocene–Oligocene transition. Although low in diversity, the well-preserved bryozoan fauna includes four new species and one new genus, all with discoidal or conical colony forms that were either free-living (as in *Heteractis tanzaniensis* sp. nov.) or anchored by rootlets (as in *Bragella pseudofedora* gen. et sp. nov., *Lacrimula kilwaensis* sp. nov. and

L. crassa sp. nov.) allowing them to live on a soft, unstable seafloor without the need of large substrates for attachment.

Geological setting

Within southern Tanzania, Late Cretaceous to Palaeogene marine sediments crop out along a broad coastal belt, south of the Rufiji river, from Kilwa Peninsula to Lindi Creek (Nicholas *et al.* 2006; Fig. 1A). These sediments are formally defined as the Kilwa Group, which comprises a generally homogenous sedimentary package, largely of clays and claystones to marls, that accumulated during a period of increased subsidence in the region (Nicholas *et al.* 2006). The Kilwa Group is divided into four formations: the Nangurukuru (Upper Cretaceous), Kivinje (Paleocene to lower Eocene), Masoko (middle Eocene) and Pande (upper Eocene to lower Oligocene) formations. The Pande Formation contains an apparently conformable succession across the EOB, and is intermittently exposed on a hillside close to the village of Pande in the Kilwa administrative district. The succession is expanded in comparison to other EOB reference sections, is rich in microfossils (Pearson *et al.* 2008; Wade & Pearson 2008), and provides an opportunity to study biotic changes across the EOB.

The Pande Formation is primarily a succession of dark greenish grey clays containing <10% $CaCO_3$ (Nicholas *et al.* 2006). The sedimentary facies and presence of typical bathyal smaller benthic foraminifera with diverse planktonic foraminifera suggest the clays were deposited in an outer shelf to slope setting at about 300–500 m water depth, though

maximum depths are difficult to determine. The clays contain exceptionally well-preserved calcareous microfossils (Bown *et al.* 2008; Pearson *et al.* 2008; Wade & Pearson 2008). Secondary limestone beds, deposited allochthonously with the clays, are present throughout the succession and are rich in larger benthic foraminifera and other shallow-water organisms (Cotton & Pearson 2011). Additionally, shelf debris occurs frequently within the clays in lower concentrations, including inner shelf benthic foraminifera and larger benthic foraminifera, micro-molluscs and dasycladaceans (Cotton & Pearson 2011; Cotton *et al.* in prep.), which are thought to have been washed from the shelf during storm events. Because of this it is not always clear whether fossils found within the sediments are autochthonous or allochthonous.

Material and methods

Material for this study has been collected in 2004 and 2005 as part of the Tanzania Drilling Project (TDP), which aimed to recover the EOB succession (Nicholas *et al.* 2006; Pearson *et al.* 2008). Three sites (TDP 11, 12 and 17), positioned approximately along strike within 3 km of each other, were drilled. The Tanzanian shelf, like today, was probably very narrow and the drill sites are estimated to be approximately 50 km from the palaeoshoreline (Kent *et al.* 1971; Nicholas *et al.* 2006, 2007).

Bryozoans were found in the hemipelagic clays of TDP 17 (UTM 37L; 560539 8984483; Fig. 1A). Half-round samples from the core, approximately 10 cm in length, were

washed through a 63 μm sieve and the residues dried. Bryozoan colonies were then picked using a paintbrush under a binocular microscope.

Specimens were studied and imaged with a LEO 1455VP SEM at the Natural History Museum, London, UK (NHMUK). Measurements were made from SEM micrographs using the software ImageJ. Dimensions are given in the text as the observed range and mean value, plus/minus standard deviation (the latter two values enclosed in parentheses), and using the following abbreviations: AnL: ancestrula length; AnW: ancestrula width; AvL: avicularium length; AvW: avicularium width; OL: opesia/orifice length; OW: opesia/orifice width; OvL: ooecium length; OvW: ooecium width; ZL: autozooid length; ZW: autozooid width; N: number of colonies used; n: total number of measurements made. ZL and ZW of *Lacrimula* were measured from the exposed frontal shields of zooids from the third whorl, following Cook & Lagaaij (1976), with OL and OW measurements taken on the same zooids.

For comparative purposes the holotype of *Lacrimula burrowsi* Cook, 1966, the paratype of *L. pyriformis* Cook, 1966 from Zanzibar, and specimens of *Heteractis duclosii* (Lea, 1833) from the Eocene of Texas and Mississippi (USA) and '*Lunulites*' *rutella* Tenison Woods, 1880, from the Miocene of Victoria (Australia), were studied and figured. Through the kindness of JoAnn Sanner (Smithsonian Institution, Washington DC) we have also been able to obtain new SEM images of the hypotype of *Lunulites truncata* De Gregorio, 1890 *sensu* Canu & Bassler (1920).

Samples of all bryozoan species were analyzed mineralogically at the NHMUK. X-ray diffraction (XRD) was carried out using the diffractometer system X'Pert Pro MPD from PANalytical configured in Bragg-Brentano geometry and equipped with an X'celerator position-sensitive detector. Samples were first soaked in a dilute solution of the detergent

Quaternary-O to remove clay particles and subsequently cleaned ultrasonically. Each sample was finely ground in acetone, placed on a silicon substrate and then into the spinning sample holder of the diffractometer. The analysis was performed under Cu Kα radiation (45 kV and 40 mA) between 5˚ and 80˚ 2θ at a step size of 0.02˚. Divergence and anti-scatter slits were used at diffraction angles of (1/4)˚ and (1/2)˚ respectively. Measurement time was three hours per sample.

The stable isotope stratigraphy was constructed from overlapping intervals of TDP 12 and 17 using shells of the mixed layer planktonic foraminifera *Turborotalia ampliapertura* by Pearson *et al.* (2008) (Fig. 1B). The oxygen and carbon records are both similar to deep-sea sites and have been used to correlate the succession to the global isotope curve. The age model was created using a combination of geochemical and biostratigraphical (planktonic foraminifera and nannofossil) tie points from the clays, which correlate to global stratigraphy (Fig. 1B).

Systematic palaeontology

Order **Cheilostomata** Busk, 1852

Superfamily **Microporoidea** Gray, 1848

Family **Lunulitidae** Lagaaij, 1952

Genus *Heteractis* Gabb & Horn, 1862

Type species. *Lunulites duclosii* Lea, 1833 (= *Lunulites bouei* Lea, 1833; see Gabb & Horn 1862, p. 156); Eocene, Claiborne, Alabama, USA.

Revised diagnosis. Colony discoidal, slightly convex, often regenerated from a fragment. Ancestrula encrusting a sediment grain that becomes partially or entirely overgrown. Ancestrula surrounded by six primary autozooids plus a pair of vibracula laterally or distolaterally. Increase in number of autozooidal series achieved by bifurcation of avicularian rows with intercalation of new autozooidal rows between. Autozooids with a reduced cryptocyst and large opesia, raised distally and overlapping the next distal autozooid in series. Vibracula in radial rows alternating with rows of autozooids, increasing in size towards the edge of the colony, proximally directed. Brooding zooids not skeletally distinct. Basal surface with scattered pores, lacking sector boundaries.

Remarks. Gabb & Horn (1862) introduced the genus *Heteractis* for *Lunulites duclosii* Lea, 1833, which they regarded as a synonym of *L. bouei* Lea, 1833 (Fig. 2). The original description of the genus was based on a regenerated fragment (see Gabb & Horn 1862, pl. 20, fig. 39), precluding observation of the characteristic periancestrular budding pattern. Subsequently, Canu & Bassler (1920) and Bassler (1953) treated *Heteractis* as a synonym of *Trochopora* based on what they considered to be the diagnostic colony growth of this genus, i.e. a sequence of overgrowths above a primary disc (Cook & Chimonides 1986). Buge & Muniz (1974) resurrected *Heteractis* as a subgenus of *Lunulites* to distinguish a group of species exhibiting a distinctive pattern of increase in number of zooidal rows by intercalation between bifurcating avicularian rows. They grouped together *L. bouei* and *L. truncata* De

9

Gregorio, as previously suggested by Cheetham (1966, p. 30), as well as their new species, *L. barbosae* from the Paleocene of Brazil. De Gregorio (1890, p. 31) considered *Lunulites truncata* as a variety of *L. bouei*, claiming to have observed all intermediate stages between the two forms. Although excluded by De Gregorio, it is likely that the description of *L. bouei* var. *truncata* was based on worn specimens, abraded or somehow deprived of the top, as is apparent from his original drawings (pl. 41, figs 39–46) and can be observed in Canu & Bassler's (1920) hypotype of the species (Fig. 3) in which the quartz grain originally encrusted is exposed. The same specimen shows also that the colony and zooidal characters are different from those of *L. duclosii* and more similar to those of true species of *Lunulites*. Unequivocal attribution of the Brazilian species to *Heteractis* is not possible as only regenerated fragments that lack early astogenetic stages are known. On the other hand, based on the revised diagnosis of the genus, in which we consider the early astogeny and the pattern of increase in number of autozooidal series as fundamental diagnostic characters, *'Lunulites' rutella* Tenison Woods, 1880, from the Miocene of Victoria (Australia) is here regarded, provisionally at least, as an additional species of *Heteractis* and the new combination *H. rutella* comb. nov. (Fig. 4) is proposed. Cook & Chimonides (1985a, p. 352) redescribed the Australian species pointing out the apparent uniqueness of its early budding pattern. Subsequently, Bock & Cook (1999, p. 417) highlighted the need of a generic revision for *'L.' rutella* because of its early astogeny, which clearly distinguishes the species from all other species of *Lunulites*. However, *'L.' rutella* differs from the type species of *Heteractis* (Fig. 2B) in having an ancestrula larger than later autozooids (Fig. 4C), periancestrular vibracula placed laterally instead of distolaterally with the rostrum pointing towards the distolateral corners of the ancestrula instead of a proximolateral orientation (Fig. 4B), and numerous

10

septular pores instead of a single pore (Fig. 4D). Furthermore, this species seems to lack intramural kenozooids.

Among lunulitiform genera, *Heteractis* shows some similarities in the general appearance of the colony and zooids to *Kausiaria* Bock & Cook, 1998, with which it also shares the presence of six primary autozooids alternating with small distolateral avicularia, although avicularia are absent from the periancestrular ring of *Kausiaria*, and the subsequent budding may be radial or a combination of curved, spiral and radial. In *Otionellina* Bock & Cook, 1998 the ancestrula buds one, occasionally two, distal and one proximal avicularia, followed by radial budding of autozooids (Bock & Cook 1998).

Distribution. Eocene (Bartonian) of Alabama, Texas and Mississippi (USA); Oligocene (Rupelian) of Tanzania; middle Miocene to early Pliocene of Victoria, Australia.

Heteractis tanzaniensis sp. nov.

(Figs 5, 6)

Diagnosis. Colony small, discoidal, convex. Ancestrula with two small distolateral vibracula and six periancestrular autozooids. Increase in autozooidal series achieved by bifurcation of avicularian rows and intercalation of new autozooidal rows between. Autozooids arranged in radial rows with the distal margin overlapping the next distal autozooid in series. Cryptocyst coarsely granular, narrow, widest proximally, tapering distally. Opesia occupying two-thirds of zooid length. Intramurally budded kenozooids routinely present in older autozooids and vibracula. Vibracula interzooidal, arranged in radial rows alternating with autozooidal rows,

arrowhead-shaped with a medial indentation at the opesia end and a rounded rostrum, proximally directed. Basal surface with scattered pores, lacking sector boundaries.

Etymology. Named after the east African country Tanzania.

Material. Holotype: NHMUK PI BZ 7785. Paratypes: NHMUK PI BZ 7786, 7789.

Description. Colony discoidal, slightly convex, small, 1.5–2.5 mm (N 5) in diameter (Fig. 5A). Ancestrula small (AnL 195–230 [211±18] µm, AnW 149–166 [156±9] µm, N 5), rounded rectangular, similar in appearance to later autozooids, with a coarsely granular cryptocyst sloping inwards, broader proximally, tapering laterally and reduced to a raised, narrow rim distally (Fig. 5B, C); opesia large (OL 108–158 [135±25] µm, OW 89–130 [110±20] µm, N 5), plectrum-shaped. Periancestrular ring formed by paired vibracula, small, 50–60 µm long by 30–40 µm wide (N 5, n 10), distolaterally placed with the rounded rostrum pointing towards the distolateral margins of the ancestrula, and six primary autozooids oriented radially (Fig. 5B). First-budded autozooid placed distally, slightly smaller (ZL 160–200 [180±20] µm, ZW 149–165 [156±8] µm, N 5, n 15; mean L/W 1.15) than the succeeding pair of distolateral autozooids; the subsequent proximolateral pair and proximal autozooid similar in size to later autozooids. Increase in autozooidal series achieved by bifurcation of avicularian rows and intercalation of a new autozooidal row in the fork (Fig. 5D). Autozooids arranged in radial rows, rounded polygonal with a raised distal margin overlapping the proximal part of the next distal autozooid in the series, almost as long as wide (ZL 177–254 [224±21] µm, ZW 177–255 [212±20] µm, N 5, n 30; mean L/W 1.05). Cryptocyst coarsely

granular, descending, broader proximally, tapering laterally, reduced to a narrow rim distally. Cryptocyst extensive at the bifurcation of avicularian rows owing to fusion of avicularian cryptocyst with the proximal cryptocyst of the interposed zooid (Fig. 5D). Opesia large, occupying two-thirds of zooidal length (OL 161–223 [186±18] μm, OW 116–162 [140±13] μm, N 5, n 30), oval, and usually filled by an intramural kenozooid in the ancestrula, first and sometimes second generation of zooids and avicularia (Fig. 5B). Intramural kenozooids smoothly calcified with a small circular or elliptical opening marked by a distinctive rim (Fig. 5B), deeply inset. A single, central, circular areolar pore, about 20 μm in diameter, and a pair of muscle scars visible in later autozooids (Fig. 5D, G). Vibracula interzooidal, with a granular cryptocyst best developed in those at the edge of the colony, arranged in radial rows alternating with autozooids, increasing in size towards the edge of the colony (AvL 100–167 [131±20] μm, AvW 70–106 [82±10] μm, N 5, n 20), arrowhead-shaped, with a medial indentation at the opesia end and a rounded rostrum proximally directed (Fig. 5F, G). Brooding zooids not recognized. Basal surface coarsely granular, with scattered circular pores, small, about 10 μm in diameter, usually lacking sector boundaries which become visible only in worn specimens (Fig. 6A, B).

Remarks. This new species differs from the type species, *Heteractis duclosii*, in having smaller colonies, smaller autozooids, the intramural kenozooids leaving a circular (Fig. 5B) instead of a trifoliate or slit-like opening (Fig. 2D) in later autozooids, and the arrowhead-shaped vibracula (Fig. 5E) instead of those teardrop-shaped in *H. duclosii* (Fig. 2E).

It is worth remarking about the interpretation of the intramural kenozooids as these provide a useful taxonomic character. Similar structures have been interpreted as closure

plates, i.e. calcareous walls produced in late ontogeny by the zooid to seal-off the zooidal chamber. Closure plates are generally formed at the level of the mural rim and often contain moulds of the opercular sclerites near the distal end (e.g. *Reptoporina micropora*, see Gordon & Taylor (2005), p. 85, fig. 1F–H; *Electra everretti*, see Taylor & McKinney (2006), p. 242, pl. 37, fig. 1e). In contrast, the structures in *Heteractis* lack impressions of the operculum and, importantly, are located well below the level of the mural rim. They are therefore better interpreted as kenozooids budded within the moribund host zooid. Such intramural kenozooids are widespread among anascan cheilostomes (e.g. *Pyriflustrina elegans*, see Gordon & Taylor (2005), p. 85, fig. 1B; *Pyrisinella meniscacantha*, see Taylor & McKinney (2006), p. 281, pl. 76, fig. 1a), and represent a primitive character that appeared early in cheilostome evolution at least since the Late Cretaceous (Taylor 1988; Gordon & Taylor 2005; Taylor & McKinney 2006).

Although brooding zooids are not clearly distinguishable, at the periphery of some colonies a few zooids with disproportionately larger opesia were observed (Fig. 5G). These are conceivably brooding zooids, although they may simply be zooids that are large because of the geometry of increased row width in the growing colony. Peripheral polymorphs with enlarged opesia are involved in reproduction in several lunulitid genera such as *Otionella* and *Selenaria* (Chimonides & Cook 1981; Cook & Chimonides 1985a, b).

A grain of quartz is often visible partially embedded on the centre of the basal surface of the colony (Fig. 6). In other sexual colonies the substrate is not visible, which may indicate that it has been totally overgrown.

Superfamily **Mamilloporoidea** Canu & Bassler, 1927

Family **Ascosiidae** Jullien, 1883

Genus ***Bragella*** gen. nov.

Type species. *Bragella pseudofedora* sp. nov.; Oligocene, Rupelian, Tanzania.

Diagnosis. Colony stellate or lenticular, flat. Ancestrula similar to later autozooids but smaller and surrounded by five periancestrular zooids. Autozooids with nodular frontal shield, imperforate except for a few marginal areolar pores. Orifice cleithridiate (keyhole-shaped) with distinct condyles, arched anter and bowl-shaped poster. Oral spines present only in ancestrula and periancestrular zooids. Avicularia inconstant, adventitious, derived from lateral areolar pores. Kenozooids intramural and frontally budded, the latter occupying the central part of the colony, obscuring the ancestrula and early astogeny. Ovicells unknown. Basal surface convex with clearly defined zooidal boundaries and pores.

Etymology. Named to honour recently deceased palaeobryozoologist Prof. Giampietro Braga.

Remarks. This new genus is introduced to allocate a new species (see description below) showing a mixture of characters reminiscent of other taxa. The lenticular shape of the colony characterized by a low profile occurs in certain species of the conescharellinid genera *Conescharellina* (e.g. *C. perculta* and *C. plana*) and *Trochosodon* (e.g. *T. ampulla*, *T. diommatus* and *T. aster*). As in *Conescharellina*, the new genus is characterized by ontogenetic changes involving the development of secondary calcification by frontal budding

15

of kenozooids that occupy the central part of the colony and obscure early astogenetic features. However, all genera of Conescharellinidae are characterized by reversed frontal budding, which does not occur in *Bragella* gen. nov.

Although the overall morphology of *Bragella* – including the tuberculate frontal shield, the apparent lack of ovicells, the shape of the orifice and the placement of avicularia – closely resembles *Fedora*, the characteristic distobasal pore chambers of this genus are lacking. *Ascosia* has flat colonies and lacks distobasal pore chambers but differs from *Bragella* in having suberect zooids.

Placement of *Bragella* in Ascosiidae is tentative. Although *Bragella* fits in the revised diagnosis of the family given by Gordon & d'Hondt (1997, p. 49) because of its discoidal colonies, zooids with imperforate frontal shield radiating from the central ancestrular region, orifice with condyles and broad poster, and avicularia adjacent to the orifice, genera included in Ascosiidae lack oral spines, have avicularia with complete cross-bars, and a concave basal surface.

Bragella pseudofedora sp. nov.

(Fig. 7)

Diagnosis. See genus.

Etymology. Referring to its apparent similarity with certain species of the genus *Fedora*.

Material. Holotype: NHMUK PI BZ 7790. Paratypes: NHMUK PI BZ 7791, 7792.

Description. Colony small, stellate or triangular in early astogenetic stages (Fig. 7A) to lenticular in later development (Fig. 7E), flat, 0.8–1.7 mm (N 8) in diameter. Ancestrula similar to later autozooids but smaller (AnL 314–379 [346±46] μm, AnW 303–337 [320±24] μm, N 3), with at least four oral spine bases, 15–20 μm in diameter, and surrounded by five periancestrular zooids oriented radially (Fig. 7B). Autozooids rounded polygonal, longer than wide (ZL 329–540 [446±67] μm, ZW 286–434 [348±49] μm, N 8, n 15; mean L/W 1.28). Frontal shield nodular, imperforate apart from 1–3 circular areolar pores, about 30 μm in diameter, randomly placed along zooidal margins (Fig. 7C, D). Primary orifice elongated (175–210 [190±14] μm long by 140–150 [146±4] μm wide, N 8, n 10), cleithridiate, a pair of small, rounded condyles placed at one-third of its length separating a horseshoe-shaped anter from a broad, bowl-shaped poster (Fig. 7C). Oral spine bases, numbering 2–4, restricted to periancestrular zooids. Avicularia adventitious, inconstant, usually single, large (AvL 156–235 [189±25] μm, AvW 92–177 [149±27] μm, N 6, n 8), placed laterally of autozooidal orifice, subtriangular with a rounded rostrum pointing proximally, and possibly two faint condyles (Fig. 7C). Intramural budded kenozooids often replacing avicularia, and appearing as a swollen, smooth calcification with a sunken, circular pit at the centre (Fig. 7D). Ovicells not observed. Frontally budded kenozooids occupying the central core of the colony, often obscuring ancestrula and periancestrular zooids (Fig. 7E). Basal surface convex with shallow furrows coinciding with zooidal boundaries and a single pore (about 20 μm in diameter) per zooid located at about mid-length (Fig. 7F), possibly representing rootlet pores.

Remarks. See genus.

Superfamily **Conescharellinoidea** Levinsen, 1909

Family **Batoporidae** Neviani, 1901

Genus *Lacrimula* Cook, 1966

Lacrimula kilwaensis sp. nov.

(Fig. 8)

Diagnosis. Colony elongated, conical to pear-shaped, consisting of 4–7 alternating whorls of up to 6 zooids each. Adapical kenozooidal tube reticulate and evenly porous. Zooids with reticulate, imperforate frontal shield. Marginal areolar pores present. Orifice with condyles, arched anter and wide bowl-shaped poster. Interzooidal avicularia restricted to the adapical region, adapically directed, with elongated pointed condyles. Ovicells occurring in the proliferal and subproliferal region, reticulate and imperforate.

Etymology. Alluding to Kilwa, the administrative district of the type locality.

Material. Holotype: NHMUK PI BZ 7793. Paratypes: NHMUK PI BZ 7794, 7795, 7796, 7797, 7798, 7799.

Description. Colony small, elongated conical to pear-shaped (Fig. 8A, H), 1–2 mm long by 0.8–1.2 mm wide (N 10) at the colony proliferal region, slender (mean L/W 1.5), and consisting of 4–7 (commonly six) alternating whorls of up to 6 zooids each. Ancestrular area adapical, formed by an external, hollow tube, ornamented by a pattern of polygonal reticulate ridges (Fig. 8C, D), 120–220 μm in length by 180–285 maximum width (N 10), tapering

18

proximally with the apical aperture 110–150 μm wide, and consisting of 4–6 alternating rows of kenozooids, commonly five, externally distinguishable as circular, funnel-shaped pores, 20–30 μm in diameter. Zooids hexagonal or rhomboidal (Fig. 8B), increasing in size towards the budding zone (ZL 207–312 [265±31] μm, ZW 231–362 [293±38] μm, N 10, n 30). Frontal shield convex, ornamented with similar polygonal reticulate ridges to those of the kenozooidal tube, smooth, imperforate except for a few, circular marginal areolar pores, 16–34 μm in diameter, 2–4 visible at the corners of zooids located in the central whorls (Fig. 8B), more numerous, up to six, along the basal grooves between zooids located at the proliferal region (Fig. 8G). Primary orifice positioned almost centrally on frontal shield, deeply immersed, with two robust, smooth, rounded, downwardly directed condyles not visible in frontal view, placed at the mid-line and separating an arched anter from a wider bowl-shaped poster (Fig. 8B). Secondary orifice transversely elliptical (OL 110–154 [135±13] μm, OW 81–126 [106±13] μm, N 10, n 20). Interzooidal avicularia restricted to the first two rows of individuals below the adapical region (Fig. 8C, D), small, rounded, 50–70 μm in diameter, with elongated pointed condyles, adapically directed, and placed at the centre of an avicularian chamber similar in shape and ornamentation to an autozooid but smaller, about 150 μm long by 200 μm wide. Adventitious, suboral avicularia absent. Ovicells occurring in the proliferal and subproliferal zone zooids, broader than long (OvL 129–251 [175±40] μm, OvW 145–296 [222±49] μm, N 3, n 10), smooth with polygonal reticulate ridges, apparently imperforate (Fig. 8E, F). Primary orifices of maternal zooids slightly larger than those of autozooids, but with a shorter anter owing to the position of the condyles placed at one-third of orifice length and characterized by a straight adapical margin (Fig. 8E).

Remarks. Four fossil and five modern species have been assigned to *Lacrimula*. The geologically oldest known occurrence is *L. perfecta* (Accordi, 1947) from the Priabonian (late Eocene) of Italy. A middle Oligocene species, *L. borealis* Cook & Lagaaij, 1976, was reported from a well in the North Sea, while two Miocene species, *L. asymmetrica* Cook & Lagaaij, 1976 and *L. grunaui* Cook & Lagaaij, 1976, were described from Madura (Indonesia). Recent species are from eastern Australia (*L. affinis* Bock & Cook, 2004), Zanzibar (*L. burrowsi* Cook, 1966 and *L. pyriformis* Cook, 1966), Madura (*L. similis* Cook & Lagaaij, 1976), and India (*L. visakhensis* Rao & Rao, 1973). The new species is very similar in appearance to the western Indian Ocean *L. burrowsi* (Fig. 9A–D) and *L. pyriformis* (Fig. 9E–H), differing principally in the size of the colony, which is smaller, and consequently has fewer whorls of zooids. The new species also differs from *L. burrowsi* in having smaller imperforate ooecia and in the distribution of the avicularia – these are confined to two circles surrounding the base of the kenozooidal tube in *L. kilwaensis* sp. nov., while avicularia are regularly placed between the zooids in *L. burrowsi* (Fig. 9A). Although fairly robust in *L. kilwaensis* sp. nov., condyles in *L. burrowsi* are much stouter. *Lacrimula pyriformis* has smaller orificial condyles as well as fewer and more widely spaced pores on the apical tube (Fig. 9F). *Lacrimula affinis*, which derives its specific name from the general similarities with *L. burrowsi*, differs in having adventitious oral and antapical avicularia with a complete cross-bar. The Eocene *L. perfecta* has larger colonies and avicularia with complete cross-bars that are regularly placed between the autozooids.

Lacrimula crassa sp. nov.

(Fig. 10)

20

Diagnosis. Colony squat, cup-shaped, consisting of 4–5 alternating whorls of up to 8 zooids each. Adapical, kenozooidal tube solid, smooth, porous. Zooids with tubercular frontal shield imperforate except for a few marginal areolar pores. Orifice with faint condyles, an arched anter and a wide bowl-shaped poster. Small polymorphs interpreted as kenozooids irregularly scattered among autozooids. Clusters of small polymorphs, interpreted either as interzooidal avicularia with paired condyles or kenozooids, at the antapical surface. Ovicells occurring in the proliferal and subproliferal region.

Etymology. From the Latin adjective *crassus, -a, -um* meaning 'stout, bulky', referring to its squat colonies.

Material. Holotype: NHMUK PI BZ 7800. Paratypes: NHMUK PI BZ 7801, 7802, 7803, 7804.

Description. Colony small, cup-shaped (Fig.10A), 0.7–1.0 mm long by 0.9–1.2 mm wide (N 10), squat (mean L/W 0.7), and consisting of 4–5 alternating whorls of up to 8 zooids each. Ancestrular area adapical, formed by an external, hollow cone (Fig. 10A, B), 100–150 μm in length by 240–270 maximum width (N 10), with the apical aperture 75–105 μm wide, consisting of three alternating rows of kenozooids distinguishable as external pores variable in shape and size, first two rows of pores usually rounded and small, about 20–30 μm in diameter, third row made of larger bean-shaped pores, about 50 μm wide. Zooids hexagonal, increasing in size towards the budding zone (ZL 183–205 [191±12] μm, ZW 249–265 [255±9] μm, N 10, n 30). Frontal shield convex, tubercular (Fig. 10A, D), imperforate except

for a few, circular marginal areolar pores, 18–22 μm in diameter, 4–6 visible at the corners of zooids located in the central whorls and along the basal grooves between zooids located at the proliferal region (Fig. 10 E, G). Primary orifice positioned centrally or antapically on the frontal shield, immersed, with two faint, rounded, condyles at the mid-line (Fig. 10A, C, D) separating an arched anter from a wider bowl-shaped poster (OL 90–108 [99±13] μm, OW 87–90 [89±2] μm, N 5, n 10). Small polymorphs interpreted as kenozooids irregularly scattered among autozooids, hexagonal to trapezoidal (Fig. 10C, D), about 130 μm long by 120 μm wide, with a small, elliptical opening, slightly longer than wider, about 55–60 μm long by 50–55 μm wide, constricted at one-third of the length, antapically placed. Clusters of small polymorphs, interpreted either as interzooidal avicularia or kenozooids (Fig. 5E–H), usually five or six, located at the centre of the antapical surface. Avicularia small, rounded, 60–70 μm in diameter with a rounded rostrum outwardly directed and small, paired condyles (Fig. 10F). Ovicells occurring in proliferal and subproliferal zone zooids, large, broader than long (OvL 135–182 [167±26] μm, OvW 189–265 [213±41] μm, N 4, n 10), all observed examples either incomplete or having non-calcified ooecia frontally (Fig. 10D). Primary orifices of maternal zooids slightly larger than those of autozooids (Fig. 10D).

Remarks. This species differs from *L. kilwaensis* sp. nov. in having squatter colonies, smaller orificial condyles, small polymorphs regularly scattered within the colony, a shorter apical tube and larger avicularia clustered in the antapical surface. The general appearance of the colony closely resembles a species of *Batopora*, *B. rosula* (Reuss, 1848), from the Miocene of Europe (see Cook & Lagaaij 1976, p. 351, pl. 3, figs 2–3). The main distinction between these two batoporid genera is in the shape of the primary orifice (with condyles in

Lacrimula, without condyles in *Batopora*) and the adapical kenozooidal complex (external and tube-like in *Lacrimula*, undifferentiated and immersed as a pit in *Batopora*).

Discussion

Palaeoenvironmental significance of the Tanzanian 'sand-fauna' bryozoans

The modes of life of bryozoan species are closely reflected in the skeletal morphology of their colonies (see McKinney & Jackson 1989). Survival on unstable fine-grained sediments lacking large substrates for attachment requires the particular adaptations that are seen in so-called 'sand fauna' bryozoans. These usually have colonies that are either free-living 'lunulitiform' or rooted, including 'conescharelliniform'. Lunulitiform species are able to settle on minute sand-sized substrate that they rapidly outgrow to become free-lying discs with concave undersides and convex upper surfaces over which the feeding zooids open. The hair-like setae of their peripheral vibracular polymorphs stabilize colonies above the seafloor, while those of the centrally placed vibracula sweep away sediment particles from the upper colony surface. In contrast, rooted conescharelliniform species usually have a compact colony morphology varying in shape from globular to discoidal, conical or stellate, and are supported by kenozooidal or extrazooidal rootlets that penetrate and are attached to fine-grained sediments on the seafloor. Both free-living and rooted colony morphotypes are found on soft, unstable sea bottoms from 2 m to at least 8000 m (Cook & Chimonides 1981), with abundance peaking between about 70 and 500 m (Cook 1981).

Observations of living species allow inferences to be made on the depth and nature of the sea bottom for fossil assemblages. Cook & Lagaaij (1976) observed that as depth

23

increased the number of species adapted to fine-grained sediments increases until only bimorphic or even monomorphic assemblages remain. Our fossil assemblage is mainly made of rooted conescharelliniform and subordinate lunulitiform morphotypes. The bulk of the assemblage consists of the conescharelliniform genus *Lacrimula* in which colonies are characterized by reversed budding, i.e. the typical distal end of the orifice is closest to the proximal end of the colony. Bimorphic assemblages made of conescharelliniform along with lunulitiform species are characteristic of depths below 100 m (Cook 1981), while monomorphic assemblages of conescharelliniform species have been found in deeper waters, from 450 to 2150 m. Recent *Lacrimula* species from Zanzibar have been found at depths of 100–200 m (*L. burrowsi*) and 300–550 m (*L. pyriformis*) in muddy sediments.

The occurrence of bryozoans in the core correlates with the second isotope shift and is constrained between 33.49 Ma and 33.0 Ma (Fig. 1B), a ~500 kyr interval corresponding to the Eocene–Oligocene Glacial Maximum (EOGM). The EOGM was a global environmental change associated with the development of a major ice cap on Antarctica, cooling both globally and locally in Tanzania (Lear *et al.* 2008), and sea-level fall. It was characterized by enhanced evolutionary turnover in many biological groups on land and in the ocean, involving widespread extinction and also evolutionary innovation (Coxall & Pearson 2007). Major sea-level fall caused a global rearrangement of marine shelf and slope environments, which, together with global cooling and other environmental effects, probably had a profound influence on shallow marine biota. The deposition of bryozoan beds in several localities of northern Italy, just above the EOB and at different palaeodepths, has been interpreted as being mainly driven by a cooling of ocean waters accompanied by an increase in nutrient input into shallow environments due to changes in ocean circulation (Dunkley Jones *et al.*

24

2008b; Jaramillo-Vogel *et al.* 2013, 2016). Bryozoan marls were deposited at other localities across central Europe at about the same time (Zágoršek 1992, 1993, 1994). Likewise, James *et al.* (2016) found an increase in bryozoans across the Eocene–Oligocene boundary in sections from Kangaroo Island, South Australia.

The larger benthic foraminifera in the Tanzanian core seem to have been redeposited from shallow water, *c.* 100 m or less. The palaeoenvironment is thought to be hemipelagic, over 300 m depth, but shallow-water material from the photic zone was brought in frequently, such as the larger benthic foraminifera and dasycladaceans. As the larger benthic foraminifera and bryozoans often occur in the same samples, it could be argued that they came from the same shallow-water environment. This seems possible for the lunulitiform species *Heteractis tanzaniensis* but is less likely for *Lacrimula kilwaensis* and *L. crassa* as this genus is typical of deeper water at the present-day. Probably the bryozoan assemblage represents a mixture of depth habitats.

Palaeobiogeography of *Heteractis*

The bryozoan genus *Heteractis* is now known from three (possibly four) different geographical regions and times. The geologically oldest proven record is *Heteractis duclosii* from the middle Eocene (Lutetian–Bartonian) of southeast USA, i.e. Alabama, Texas and Mississippi (Lea 1833; Gabb & Horn 1862; Canu & Bassler 1920). Subsequently, *Heteractis* appeared in the very early Oligocene (Rupelian) of Tanzania, with *H. tanzaniensis* sp. nov. Our tentative attribution of *'Lunulites' rutella* to *Heteractis* extends its upper range to the middle Miocene–early Pliocene of Victoria, Australia (Cook & Chimonides 1985b). Requiring confirmation as a species of *Heteractis* is *H. barbosae* from northeast Brazil (Buge

& Muniz 1974), which would extend the range of the genus back to the Paleocene and shift its first appearance from the Northern to the Southern Hemisphere. Although Buge & Muniz (1974) expressed some doubts about the age of the Maria Farinha Formation from which their material came from, more recent studies have confirmed its early Paleocene age (e.g. Albertão & Martins 2006).

Whether or not the Brazilian record is accepted as *Heteractis*, a simple reading of this fossil record suggests an eastward migration of the genus through time. This can be compared with palaeobiogeographical changes in Lunulitidae as a whole. The earliest Lunulitidae appeared in Europe in the Turonian (Cook & Chimonides 1986), and remained moderately abundant and diverse in Europe and adjacent parts of Asia until their disappearance at the end of the Pliocene. In North America they became abundant in the Paleocene and had disappeared by the end of the Miocene. Lunulitidae (and related families) are restricted to Australasia at the present-day. It should be noted, however, that bryozoan faunas in some regions are still very poorly known; therefore, patterns of distribution are not necessarily a good reflection of total distribution in time or space.

Mineralogy and preservation

Cheilostome bryozoans are capable of constructing their skeletons from calcite, aragonite or a combination of these minerals, depending on the species concerned (Smith *et al.* 2006; Taylor *et al.* 2009, 2015). Aragonite is especially abundant in tropical settings (Taylor *et al.* 2016). XRD analyses undertaken of the Tanzanian core material showed two species, *Lacrimula kilwaensis* and *L. crassa*, to have monomineralic skeletons of intermediate-magnesium calcite (IMC, i.e. 4–12 mole% $MgCO_3$; see James 1997) with 4.7 mole%

MgCO$_3$. In contrast, *Bragella pseudofedora* was found to be bimineralic, with the calcite phase consisting of IMC containing 4.45 mole% MgCO$_3$, while *Heteractis tanzaniensis* is entirely aragonitic. Previous analyses performed on congeneric species revealed a bimineralic skeleton for the Recent *Lacrimula pyriformis* (Taylor *et al.* 2009) and an aragonitic skeleton for *Heteractis duclosii* (Taylor *et al.* 2014) from the Eocene.

According to Taylor *et al.* 2009, multiple clades of cheilostome bryozoans have evidently made evolutionary switchovers from entirely calcitic skeletons to skeletons containing aragonite, either alone or in combination with calcite (i.e. bimineralic). In the case of lunulite cheilostomes, it appears that the transition went from calcitic to aragonitic via an intermediate bimineralic state. The bimineralic skeleton of the late Eocene–early Oligocene species of *Lacrimula* from Tanzania compared with the aragonitic skeleton of Recent *Lacrimula* from the same area, suggests that this genus too may have changed from bimineralic to aragonitic through time, although a calcitic precursor is as yet unknown in *Lacrimula*.

Micropalaeontological sampling of bryozoans

It is known that examination of sediments for micropalaeontological purposes may reveal species of bryozoans rarely collected by conventional, macropalaeontological sampling for bryozoans (Cook 1981). 'Sand fauna' bryozoans may remain undetected or are present as accidental inclusions in Recent samples collected by grab or dredge because of their extremely minute size. Recent seafloor sediments are not routinely examined for bryozoans, and any bryozoans present may be confused with foraminifera of similar size and overall appearance. Samples of modern sea-bottom sediments collected from Zanzibar deep waters,

for instance, revealed that sand-fauna species accounted for 70–90% of the total bryozoans

present (Cook 1981). These sediments also revealed for the first time the existence of the

genus *Lacrimula*. Micropalaeontological samples of ancient sediments offer the potential for

augmenting the fossil record of bryozoans, especially in Cenozoic tropical settings from

which bryozoans are poorly known (Taylor & Di Martino 2014).

Acknowledgements

References

Accordi, B. 1947. Nuove forme di Briozoi eocenici del Veronese. *Studi Trentini di Scienze Naturali Acta Geologica*, **25**, 103–110.

Albertão, G. A. & **Martins, P. P. Jr** 2006. Limestones Strata of Poty Quarry (Paulista), State of Pernambuco – Evidences of a Catastrophic Event on the First Geological Record of the K–T Boundary in South America. Pp. 1–12 in Winge, M., Schobbenhaus, C., Berbert-Born, M., Queiroz, E. T., Campos, D. A., Souza, C. R. G. & Fernandes, A. C. S. (eds) *Geological and Palaeontological Sites of Brazil*. Available on line. http://sigep.cprm.gov.br/sitio102/sitio102english.pdf

Bassler, R. S. 1953. *Bryozoa* Vol. Part G. Pp. 1–253, in Moore R. C., Treatise on Invertebrate Paleontology. Geological Society of America and University of Kansas Press, Lawrence, Kansas.

Battistini, R., Gayet, J., Jouannic, C., Labracherie, M., Peypouquet, J. P., Pujol, C., Pujos-Lamy, A. & **Turon, J. L.** 1976. Etude des sédiments et de la microfaune des Îles glorieuses (Canal de Mozambique). *Cahiers de l'Office de la Recherche Scientifique et Technique Outre-Mer (O.R.S.T.O.M.)*, **8**, 147–171.

Bock, P. E. & **Cook, P. L.** 1998. Otionellidae, a new family including five genera of free-living lunulitiform Bryozoa (Cheilostomatida). *Memorie di Scienze Geologiche*, **50**, 195–211.

Bock, P. E. & **Cook, P. L.** 1999. Notes on Tertiary and Recent 'Lunulite' Bryozoa from Australia. *Memorie di Scienze Geologiche*, **51**, 415–430.

Bock, P. E. & **Cook, P. L.** 2004. New species of the bryozoan genera *Batopora* and *Lacrimula* (Batoporidae) from Australia. *Proceedings of the Royal Society of Victoria*, **116**, 283–288.

Bown, P. R., Jones, T. D., Lees, J., Randell, R. D., Mizzi, J. A., Pearson, P. N., Coxall, H. K., Young, J. R., Nicholas, C. J., Karega, A., Singano, J. & **Wade, B. S.** 2008. A

Paleogene calcareous microfossil Konservat-Lagerstätte from the Kilwa Group of coastal Tanzania. *Geological Society of America Bulletin*, **120**, 3–12.

Brood, K. 1976. Cyclostomatous Bryozoa from the coastal waters of East Africa. *Zoologica Scripta*, **5**, 277–300.

Buge, E. & **Muniz, G. da C. B.** 1974. *Lunulites (Heteractis) barbosae* – nouvelle espèce de bryozoaire lunulitiforme (Bryozoa, Cheilostomata) du Paléocène du nord-est du Brésil. *Annales de Paléontologie, Invertébrés, Paris*, **60**, 191–201.

Busk, G. 1852. An account of the Polyzoa, and sertularian zoophytes, collected in the voyage of the Rattlesnake, on the coasts of Australia and the Louisiade Archipelago, & c. Pp. 343–402 in J. MacGillivray (ed.) *Narrative of the Voyage of H.M.S. Rattlesnake, commanded by the late Captain Owen Stanley . . . 1846–1850; including discoveries and surveys in New Guinea, the Louisiade Archipelago, etc., to which is added the account of Mr E. B. Kennedy's expedition for the exploration of the Cape York Peninsula [including Mr W. Carron's narrative]. Volume 1.* T. W. Boone, London.

Canu, F. & **Bassler, R. S.** 1917. A synopsis of American Early Tertiary cheilostome Bryozoa. *United States National Museum Bulletin*, **96**, 1–87.

Canu, F. & **Bassler, R. S.** 1920. North American Early Tertiary Bryozoa. *United States National Museum Bulletin*, **106**, 1–879.

Canu, F. & **Bassler, R. S.** 1927. Classification of the cheilostomatous Bryozoa. *Proceedings of the United States National Museum*, **69** (14), 1–42.

Cheetham, A. H. 1966. Cheilostomatous Polyzoa from the Upper Bracklesham Beds (Eocene) of Sussex. *Bulletin of the British Museum (Natural History), Geology, London,* **13**, 1–115.

Chimonides, P. J. & **Cook, P. L.** 1981. Observations on living colonies of *Selenaria* (Bryozoa, Cheilostomata) II. *Cahiers de Biologie Marine*, **22**, 207–219.

Cook, P. L. 1966. Some "sand fauna" Polyzoa (Bryozoa) from eastern Africa and the northern Indian Ocean. *Cahiers de Biologie Marine*, **7**, 207–223.

Cook, P. L. 1981. The potential of minute bryozoan colonies in the analysis of deep sea sediments. *Cahiers de Biologie Marine*, **22**, 89–106.

Cook, P. L. & **Lagaaij, R.** 1976. Some Tertiary and recent conescharelliniform Bryozoa. *Bulletin of the British Museum (Natural History), Zoology, London*, **29**, 319–376.

Cook, P. L. & **Chimonides, P. J.** 1981. Early astogeny of some rooted cheilostome Bryozoa. Pp. 59–64 in Larwood, G. P. & Nielsen, C. (eds) *Recent and Fossil Bryozoa*. Olsen & Olsen, Fredensborg.

Cook, P. L. & **Chimonides, P. J.** 1985a. Recent and fossil Lunulitidae (Bryozoa, Cheilostomata), 5. *Selenaria alata* Tenison Woods and related species. *Journal of Natural History*, **19**, 337–358.

Cook, P. L. & **Chimonides, P. J.** 1985b. Recent and fossil Lunulitidae (Bryozoa, Cheilostomata), 4. American and Australian species of *Otionella*. *Journal of Natural History*, **19**, 575–603.

Cook, P. L. & **Chimonides, P. J.** 1986. Recent and fossil Lunulitidae (Bryozoa, Cheilostomata), 6. *Lunulites* sensu lato and the genus *Lunularia* from Australasia. *Journal of Natural History*, **20**, 681–705.

Cotton, L. J. & **Pearson, P. N.** 2011. Extinction of larger benthic foraminifera at Eocene/Oligocene boundary. *Palaeogeography, Palaeoclimatology, Palaeoecology*, **311**, 281–296.

Cotton, L. J., Arciszewski, J., Reich, S., Wesselingh, F. & **Pearson, P. N.** in prep. Micro-mollusc response to the Eocene Oligocene Transition, Kilwa District Tanzania.

Coxall, H. K. & **Pearson, P. N.** 2007. The Eocene–Oligocene transition. Pp. 351–387 in Williams, M., Haywood, A. M., Gregory, F. J. & Schmidt, D. N. (eds) *Deep-time Perspectives on Climate Change: Marrying the Signal from Computer Models and Biological Proxies*. The Micropalaeontological Society, Special Publications, London.

De Gregorio, A. 1890. *Monographie de la Faune Éocénique de l'Alabama et surtout de celle de Claiborne de l'Étage Parisien.* Annales de Géologie et de Paléontologie, Palermo, 316 pp., 46 pls

Dunkley Jones, T., Bown, P. R. & **Pearson, P. N.** 2008a. Exceptionally well preserved upper Eocene to lower Oligocene calcareous nannofossils (Prymnesiophycidae) from the Pande Formation (Kilwa group) Tanzania. *Journal of Systematic Palaeontology*, **4**, 359–411.

Dunkley Jones, T., Bown, P. R., Pearson, P. N., Wade, B. S., Coxall, H. K. & **Lear, C. H.** 2008b. Major shifts in calcareous phytoplankton assemblages through the Eocene-Oligocene transition of Tanzania and their implications for low-latitude primary production. *Paleoceanography*, **23**. doi:10.1029/2008PA001640.

Gabb, W. M. & **Horn, G. H.** 1862. The fossil Polyzoa of the Secondary and Tertiary Formations of North America. *Journal of the Academy of Natural Sciences of Philadelphia*, **5**, 111–179.

Gordon, D. P. & **Hondt, J.-L. d'** 1997. Bryozoa: Lepraliomorpha and other Ascophorina, mainly from New Caledonian waters. *Mémoires du Muséum National d'Histoire Naturelle (A)*, **176**, 9–124.

Gordon, D. P. & Taylor, P. D. 2005. The cheilostomatous genera of Alcide d'Orbigny – nomenclatural and taxonomic status. Pp. 83–97 in Moyano, G., Hugo, I., Cancino, J. M. & Wyse-Jackson, P. N. (eds) *Bryozoan Studies 2004*. Balkema, Leiden.

Gray, J. E. 1848. *List of the Specimens of British Animals in the Collection of the British Museum. Part 1. Centroniae or Radiated Animals.* Trustees of the British Museum (Natural History), London, xiii + 173 pp.

Gurgel, I. & **Vasseur, P.** 1974. Sur une collection de Bryozoaires récoltés à Ile Europe (Canal de Mozambique). *Tethys*, **5**, 337–350.

Hayward, P. J. 1988. Mauritian cheilostome Bryozoa. *Journal of Zoology, London*, **215**, 269–356.

James, N. P. 1997. The cool-water carbonate depositional realm. Pp. 1–20 in James, N. P., & Clarke, J. A. D. (eds) *Cool-water Carbonates*, SEPM Special Publication, no. 56, SEPM (Society of Sedimentary Geology), Tulsa, Oklahoma.

James, N. P., Matenaar, J. & **Bone, Y.** 2016. Cool-water Eocene–Oligocene carbonate sedimentation on a paleobathymetric high, Kangaroo Island, southern Australia. *Sedimentary Geology*. doi:10.1016/j.sedgeo.2016.04.011

Jaramillo-Vogel, D., Strasser, A., Frijia, G. & **Spezzaferri, S.** 2013. Neritic isotope and sedimentary records of the Eocene-Oligocene greenhouse-icehouse transition: The Calcare di Nago Formation (northern Italy) in a global context. *Sedimentary Geology*, **331**, 148–161.

Jaramillo-Vogel, D., Bover-Arnal, T. & **Strasser, A.** 2016. Bryozoan beds in northern Italy as a shallow-water expression of environmental changes during the Oligocene isotope event 1. *Palaeogeography, Plaeoclimatology, Palaeoecology*, **369**, 361–376.

Jullien, J. 1883. Dragages du 'Travailleur', Bryozoaires. Espèces draguées dans l'Océan Atlantique en 1881. *Bulletin de la Société Zoologique de France*, **6**, 497–534.

Keij, A. J. 1973. The bryozoan genus *Skylonia* Thomas (Cheilostomata). *Bulletin of the British Museum (Natural History), Geology Series*, **24**, 217–233.

Kent, P. E., Hunt, J. A. & **Johnstone, D. W.** 1971. *The geology and geophysics of coastal Tanzania*. Geophysical Paper No. 6, Institute of Geological Sciences, HMSO, London, 101 pp.

Kirkpatrick, R. 1888. Polyzoa of Mauritius. *Annals and Magazine of Natural History, Series 6*, **1**, 72–85.

Lagaaij, R. 1952. The Pliocene Bryozoa of the Low Countries and their bearing on the marine stratigraphy of the North Sea region. *Mededelingen van de Geologische Stichting*, **5**, 6–233.

Lea, I. 1833. *Contributions to geology*. Philadelphia, 227 pp., 6 pls

Lear, C. H., Bailey, T. R., Pearson, P. N., Coxall, H. K. & **Rosenthal, Y.** 2008. Cooling and ice growth across the Eocene–Oligocene transition. *Geology*, **36**, 251–254.

Levinsen, G. M. R. 1909. *Morphological and Systematic Studies on the Cheilostomatous Bryozoa*. Nationale Forfatteres Forlag, Copenhagen, vii + 431 pp.

McKinney, F.K. & **Jackson, J.B.C.** 1989. *Bryozoan Evolution.* Studies in Paleobiology, Unwin Hyman, Boston, 238 pp.

Neviani, A. 1901. Briozoi neogenici delle Calabrie. *Palaeontographia Italica*, **6**, 115–266.

Nicholas, C. J., Pearson, P. N., Bown, P. R., Dunkley Jones, T., Huber, B. T., Karega, A., Lees, J. A., McMillan, I. K., O'Halloran, A., Singano, J. M. & **Wade, B.S.** 2006.

Stratigraphy and sedimentology of the Upper Cretaceous to Paleogene Kilwa Group, southern coastal Tanzania. *Journal of African Earth Sciences*, **45**, 431–466.

Nicholas, C. J., Pearson, P. N., McMillan, I. K., Ditchfield, P. J. & **Singano, J. M.** 2007. Structural evolution of southern coastal Tanzania since the Jurassic. *Journal of African Earth Sciences*, **48**, 273–297.

Pearson, P. N., van Dongen, B. E., Nicholas, C. J., Pancost, R. D., Schouten, S., Singano, J. M. & **Wade, B. S.** 2007. Stable warm tropical climate through the Eocene Epoch. *Geology*, **35**, 211–214.

Pearson, P. N., McMillan, I. K., Wade, B. S., Dunkley Jones, T., Coxall, H. K., Bown, P. R. & **Lear, C. H.** 2008. Extinction and environmental change across the Eocene–Oligocene boundary in Tanzania. *Geology*, **36**, 179–182.

Pearson, P. N. & **Wade, B. S.** 2015. Systematic taxonomy of exceptionally well-preserved planktonic foraminifera from the eocene/oligocene boundary of tanzania. *Cushman Foundation for Foraminiferal Research Special Publication*, **45**, 1–85.

Rao, S. M. & **Rao, K. T.** 1973. A new bryozoan species from the shelf sediments off the east coast of India. *Current Science*, **42**, 506–507.

Reuss, A. E. 1848. Die fossilen Polyparien des Wiener Tertiärbeckens. *Naturwissenschaftliche Abhandlungen*, **2**, 1–109.

Smith A. M., Key, M. M. Jr & **Gordon, D. P.** 2006. Skeletal mineralogy of bryozoans: Taxonomic and temporal patterns. *Earth-Science Reviews*, **78**, 287–306.

Taylor, P. D. 1988. Colony growth pattern and astogenetic gradients in the Cretaceous cheilostome bryozoan *Herpetopora*. *Palaeontology*, **31**, 519–549.

Taylor, P. D. & **Di Martino, E.** 2014. Why is the tropical Cenozoic fossil record so poor for bryozoans? In Rosso, A., Wyse-Jackson, P. N. & Porter, J. S. (eds) *Bryozoan Studies 2013*, *Studi Trentini di Scienze Naturali*, **94**, 249–257.

Taylor, P. D. & McKinney, F. K. 2006. Cretaceous Bryozoa from the Campanian and Maastrichtian of the Atlantic and Gulf Coastal Plains, United States. *Scripta Geologica*, **132**, 1–346.

Taylor, P. D., James, N. P., Bone, Y., Kukliński, P. & **Kyser, T. K.** 2009. Evolving mineralogy of cheilostome bryozoans. *Palaios*, **24**, 440–452.

Taylor, P. D., James, N. P. & **Phillips, G.** 2014. Mineralogy of cheilostome bryozoans across the Eocene–Oligocene boundary in Mississippi, USA. *Palaeobiodiversity and Palaeoenvironments*, **94**, 425–438.

Taylor, P. D., Lombardi, C. & **Cocito, S.** 2015. Biomineralization in bryozoans: present, past and future. *Biological Reviews*, **90**, 1118–1150.

Taylor, P. D., Tan, S.-H. A., Kudryavstev, A. B. & **Schopf, J. W.** 2016. Carbonate mineralogy of a tropical bryozoan biota and its vulnerability to ocean acidification. *Marine Biology Research*, **12**, 776–780. doi: 10.1080/17451000.2016.1203951

Tenison Woods, J. E. 1880. On some Recent and fossil species of Australian Selenariadae (Polyzoa). *Transactions of the Royal Society of South Australia, Adelaide*, **3**, 1–12.

Thomas, H. D. 1961. Skylonia mirabilis gen. et sp. nov., a problematical fossil from the Miocene of Kenya. *Annals and Magazine of Natural History, Series 13*, **4**, 359–363.

Wade, B. S. & **Pearson, P. N.** 2008. Planktonic foraminiferal turnover, diversity fluctuations and geochemical signals across the Eocene/Oligocene boundary in Tanzania. *Marine Micropaleontology*, **68**, 244–255.

Waters, A. W. 1913. The marine fauna of British East Africa and Zanzibar, from collections made by Cyril Crossland M.A., B. Sc., F.Z.S., in the years 1901–1902. Bryozoa – Cheilostomata. *Proceedings of the Zoological Society of London*, **1913**: 458–537.

Waters, A. W. 1914. The marine fauna of British East Africa and Zanzibar, from collections made by Cyril Crossland M.A., B. Sc., F.Z.S., in the years 1901–1902. Bryozoa – Cyclostomata, Ctenostomata, and Endoprocta. *Proceedings of the Zoological Society of London*, **1914**: 831–858.

Zágoršek, K. 1992. Priabonian (Late Eocene) Cyclostomata Bryozoa from the Western Carpathians (Czechoslovakia). Geologica Carpathica, **43**, 235–247.

Zágoršek, K. 1993. Changes in Bryozoa community in the Upper Eocene sequence of Matyashegy (Hungary). *Öslénytani Viták (Discussiones Paleontologicae)*, **39**, 91–96.

Zágoršek, K. 1994. Late Eocene (Priabonian) Cheilostomata Bryozoa from Liptov Basin — Western Carpathians (Slovakia). *Neues Jahrbuch für Geologie und Paläontologie. Abhandlungen*, **193**, 361–382.

Figure captions
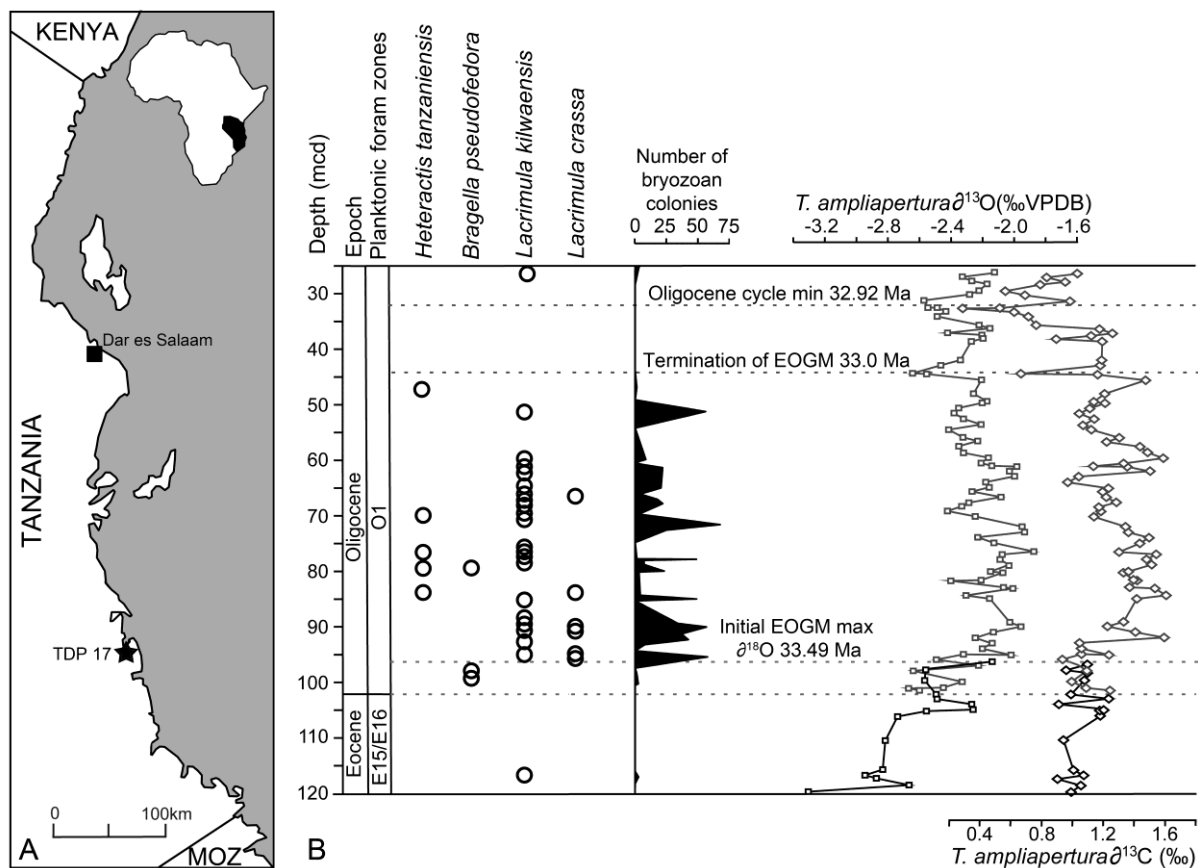
Figure 1. A, location of the Tanzanian Drilling Project Eocene–Oligocene boundary site

TDP 17; **B,** bryozoan occurrences and abundance in TDP 17 samples plotted against isotope

data from Pearson *et al.* 2008 (in grey, isotope records from TDP 17; in black isotope records

from a further site, TDP 12); EOGM = Eocene–Oligocene Glacial Maximum; mcd = mean

composite depth; MOZ = Mozambique.
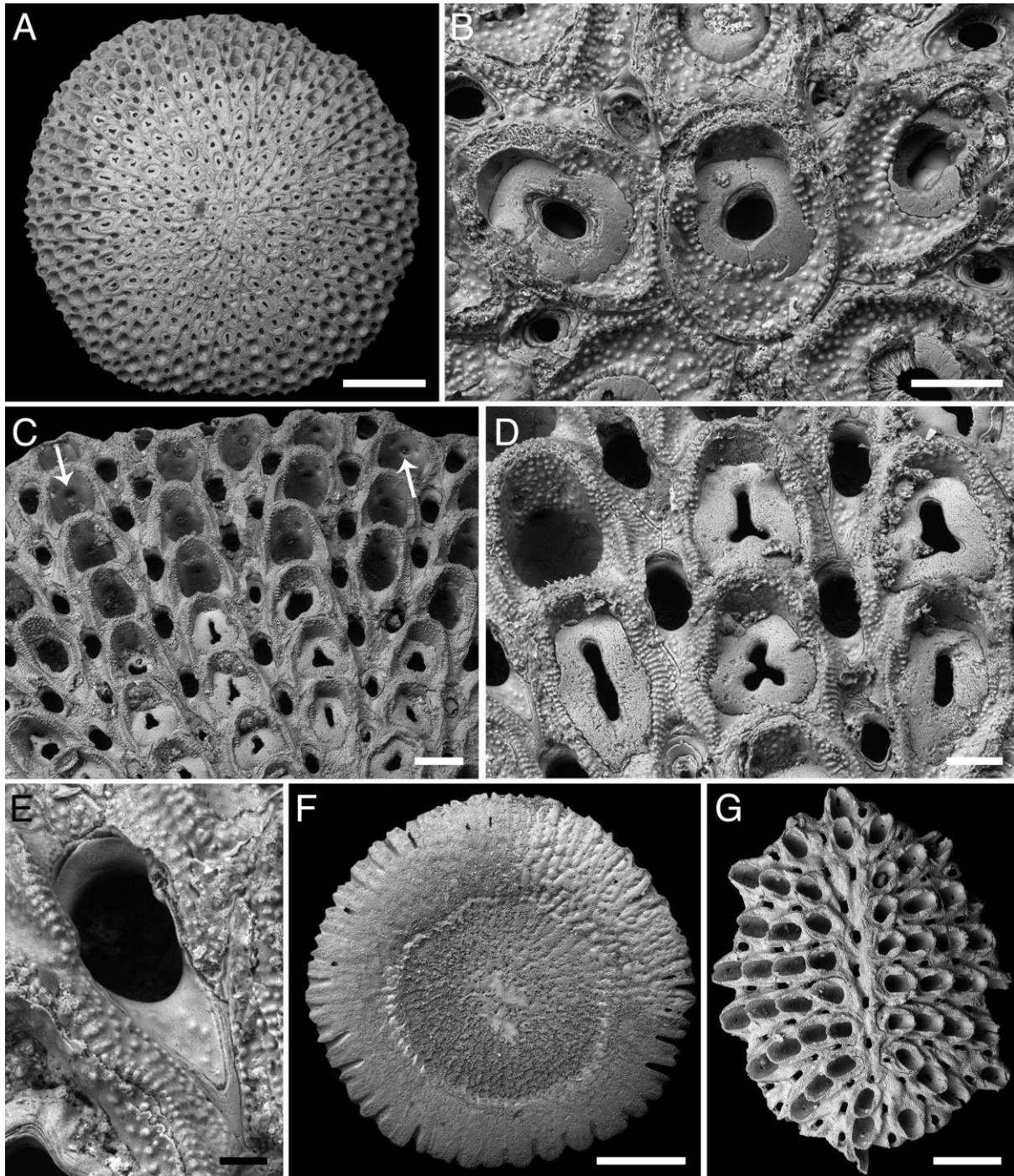
Figure 2. A–F, *Heteractis duclosii* (Lea, 1833), NHMUK PI BZ 4121, Eocene, Bartonian, L. Claiborne, Elm Creek, Lee County, Texas, USA; **A,** general view of the colony; **B,** close-up of the ancestrula with distolateral vibracula and intramural kenozooids; **C,** radial series of autozooids alternating with vibracula; note the insertion of autozooidal rows at the

bifurcation of avicularian rows. Septular pores are indicated by arrows; **D,** group of autozooids and vibracula; note the variation in shape of the closure plate openings; **E,** close-up of a vibraculum with teardrop-shaped rostrum; **F,** view of the basal surface. **G,** NHMUK PI BZ 5952, Eocene, late Bartonian, Moodys Branch Fm., LeFleur's Bluff, MMNS, Jackson, Mississippi, USA, asexual colony, the narrow vertical zone of zooids at the centre representing the fragment of the original colony from which regeneration occurred. Scale bars: A, F = 1 mm; B, D = 100 μm; C = 200 μm; E = 40 μm; G = 500 μm.
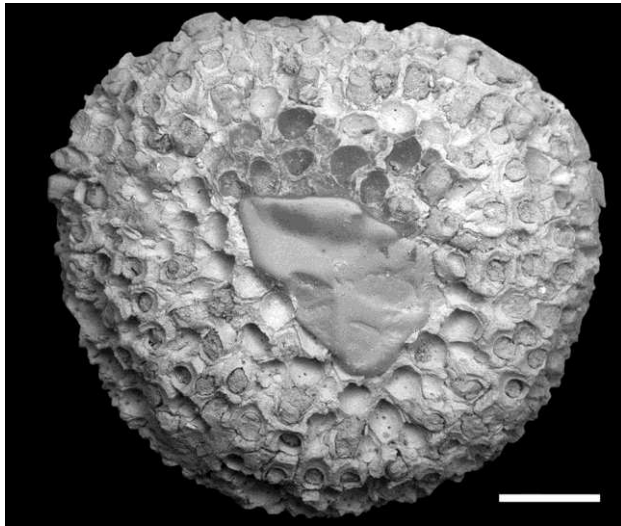
Figure 3. *Lunulites truncata* De Gregorio, 1890, hypotype, USNM 63838, middle Eocene, Claibornian, Claiborne, Alabama, USA, general view of the colony. Scale bar: 500 μm.
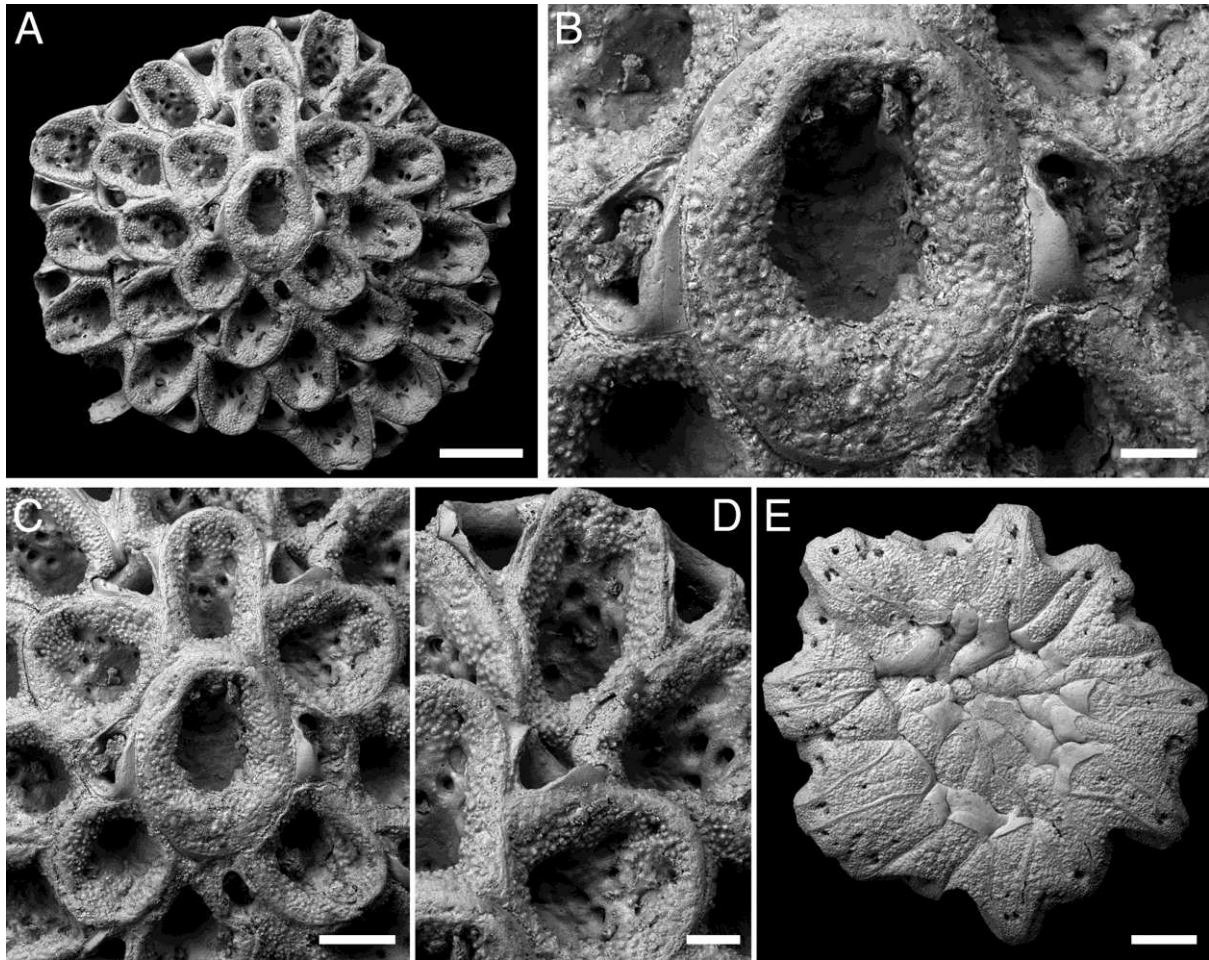
Figure 4. *Heteractis rutella* (Tenison Woods, 1880) comb. nov., NHMUK D53545, Miocene, Clifton Bank, Muddy Creek, Victoria, Australia; **A,** general view of the colony; **B,** close-up of the ancestrula flanked by a pair of vibracula; **C,** ancestrula and early astogeny; **D,** close-up of an autozooid at the bifurcation of avicularian rows; **E,** view of the basal surface. Scale bars: A, E = 500 μm; B, D = 100 μm; C = 200 μm.
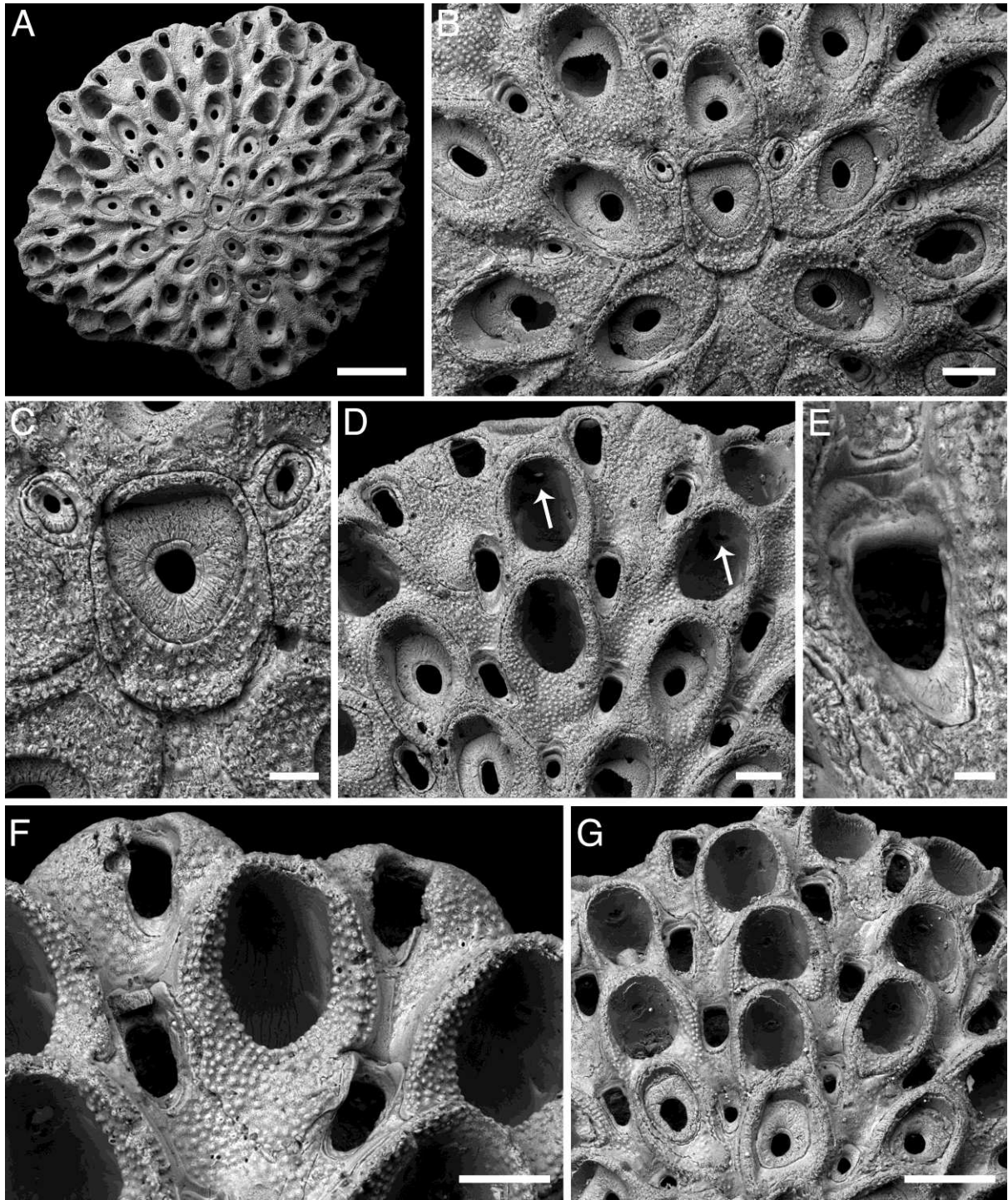
Figure 5. *Heteractis tanzaniensis* sp. nov., Oligocene, Rupelian, TDP 17, Pande Peninsula, Kilwa District, Tanzania; **A–F,** holotype, NHMUK PI BZ 7785; **A,** general view of the colony; **B,** ancestrula and early astogeny; **C,** close-up of the ancestrula, with opesia occupied

by an intramurally budded kenozooid, and a pair of distolateral vibracula also with intramural kenozooids; **D,** radial series of autozooids alternating with vibracula; note the insertion of a new autozooidal row (centre) at the bifurcation of an avicularian row. Septular pores are indicated by arrows; **E,** close-up of a vibraculum; note the medial indentation at the opesia end and the rounded rostrum; **F,** vibracula at the colony edge. **G,** paratype, NHMUK PI BZ 7786, group of zooids, some having larger opesia with straight proximal margins (brooding zooids?). Scale bars: A = 400 μm; B, D, F = 100 μm; C = 50 μm; E = 20 μm; G = 200 μm.
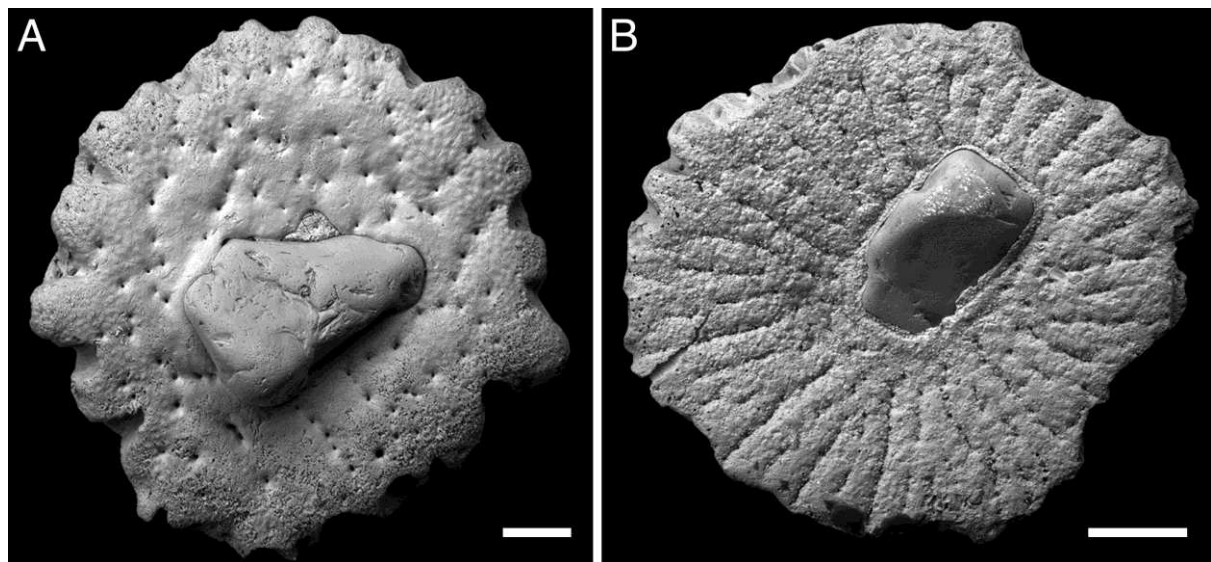

Figure 6. *Heteractis tanzaniensis* sp. nov., Oligocene, Rupelian, TDP 17, Pande Peninsula, Kilwa District, Tanzania; basal surfaces of colonies and partly enveloped sediment grain substrates. **A,** paratype, NHMUK PI BZ 7789, basal surface with scattered pores. **B,** holotype, NHMUK PI BZ 7785, basal surface with pores and sector boundaries. Scale bars: A = 200 μm; B = 500 μm.
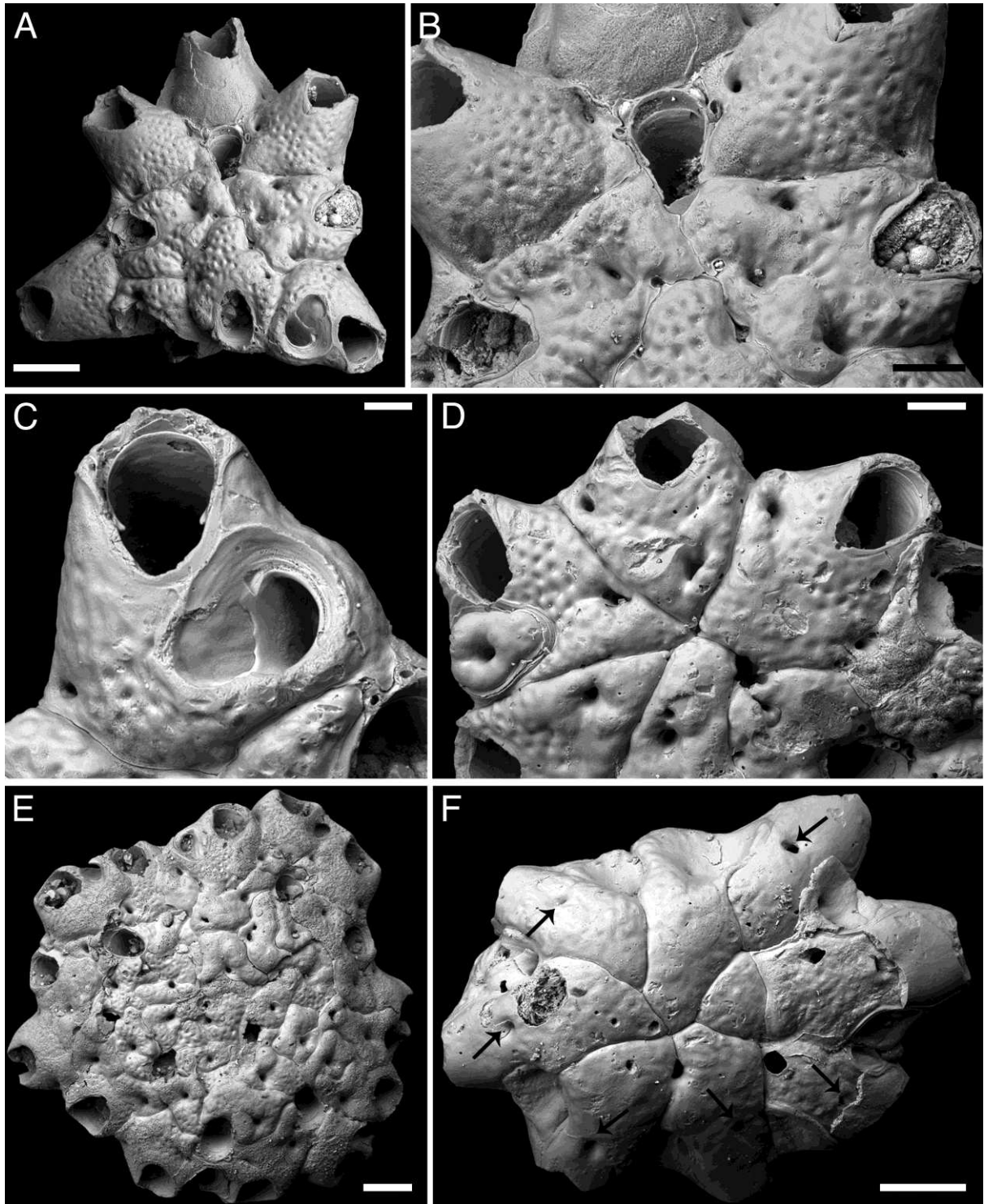
Figure 7. *Bragella pseudofedora* sp. nov., Oligocene, Rupelian, TDP 17, Pande Peninsula, Kilwa District, Tanzania. **A–C**, holotype, NHMUK PI BZ 7790; **A,** general view of the colony; **B,** ancestrula (centre) with four oral spine bases; **C,** close-up of an autozooid,

showing the cleithridiate orifice, and an adventitious avicularium. **D,** paratype, NHMUK PI BZ 7791, group of zooids; note avicularium (left) with an intramurally budded kenozooid. **E,** paratype, NHMUK PI BZ 7792, lenticular colony with frontally budded kenozooids overgrowing earlier zooids. **F,** paratype, NHMUK PI BZ 7791, view of the basal surface with zooidal boundaries and a single pore per zooid (indicated by arrows). Scale bars: A, E, F = 200 μm; B, D = 100 μm; C = 50 μm.
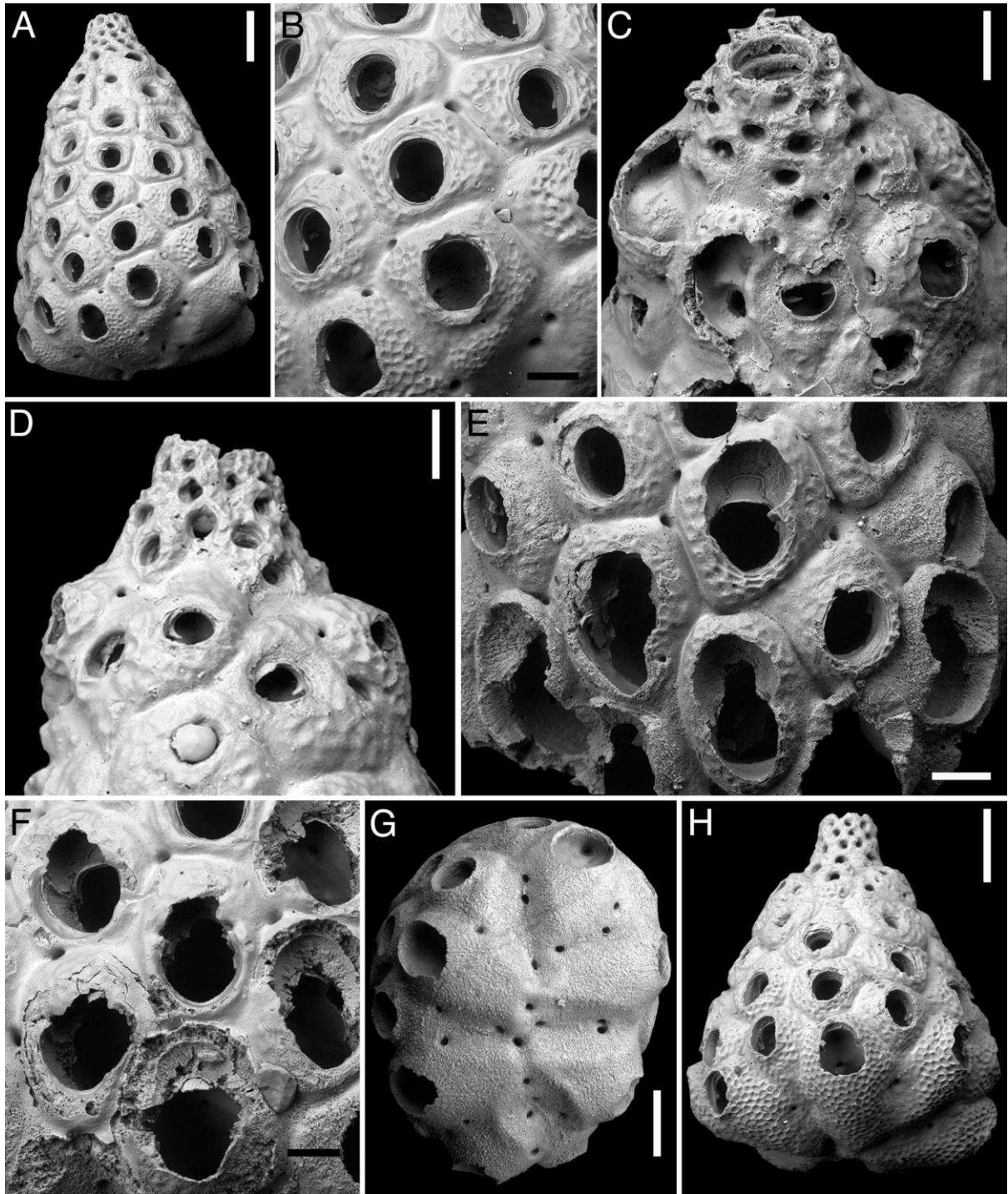
Figure 8. *Lacrimula kilwaensis* sp. nov., Oligocene, Rupelian, TDP 17, Pande Peninsula,

Kilwa District, Tanzania. **A, B,** holotype, NHMUK PI BZ 7793; **A,** general view of the

colony; **B,** group of autozooids showing orificial condyles. **C,** paratype, NHMUK PI BZ

7794, view of the opening of the adapical kenozooidal tube. **D,** paratype, NHMUK PI BZ 7795, interzooidal avicularia with well-developed, sharp condyles. **E,** paratype, NHMUK PI BZ 7796, group of ovicellate zooids at the proliferal region; note the straight adapical margin of the orifice. **F,** paratype, NHMUK PI BZ 7797, group of ovicellate zooids. **G,** paratype, NHMUK PI BZ 7798, view of the antapical surface of the colony. **H,** paratype, NHMUK PI BZ 7799, colony showing clearly the zooidal frontal shield ornamented with polygonal reticulate ridges. Scale bars: A, G, H = 200 μm; B, C, D, E, F = 100 μm.
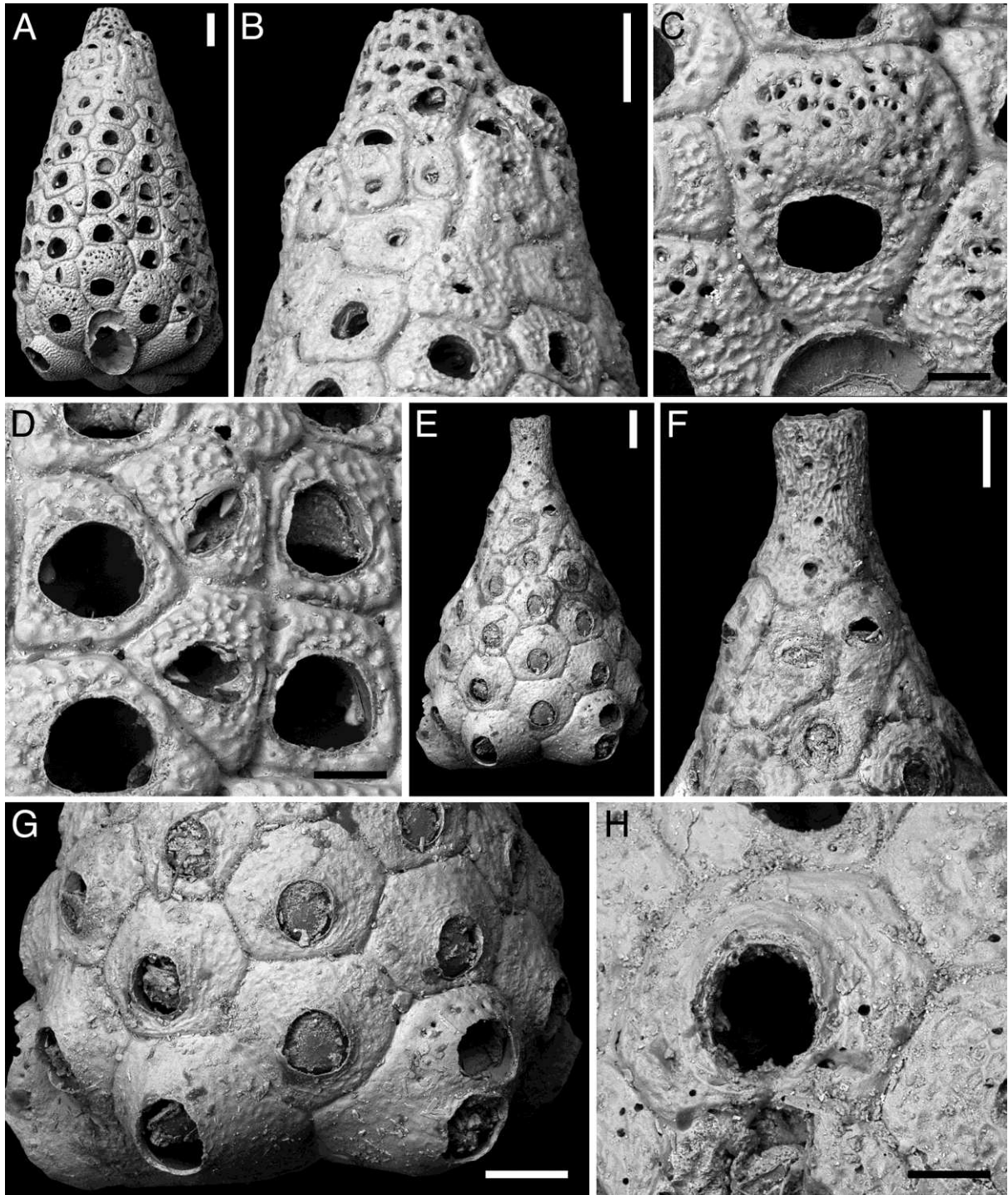
Figure 9. A–D, *Lacrimula burrowsi* Cook, 1966, holotype, NHMUK 1965.8.24.7, Recent, Station 103, J. Murray Collection, Zanzibar; **A,** general view of the colony; **B,** view of the adapical, kenozooidal tube; **C,** close-up of an ovicellate zooid; **D,** interzooidal avicularia and

autozooids. **E–H,** *Lacrimula pyriformis* Cook, 1966, paratype, NHMUK 1965.8.24.13,

Recent, Station 105, J. Murray Collection, Zanzibar; **E,** general view of the colony; **F,** view

of the adapical, kenozooidal tube; **G,** group of zooids, one with a broken ovicell; **H,** close-up

of an autozooid; a condyle is visible inside the orifice in oblique view. Scale bars: A, B, E, F,

G = 200 μm; C, D, H = 100 μm.
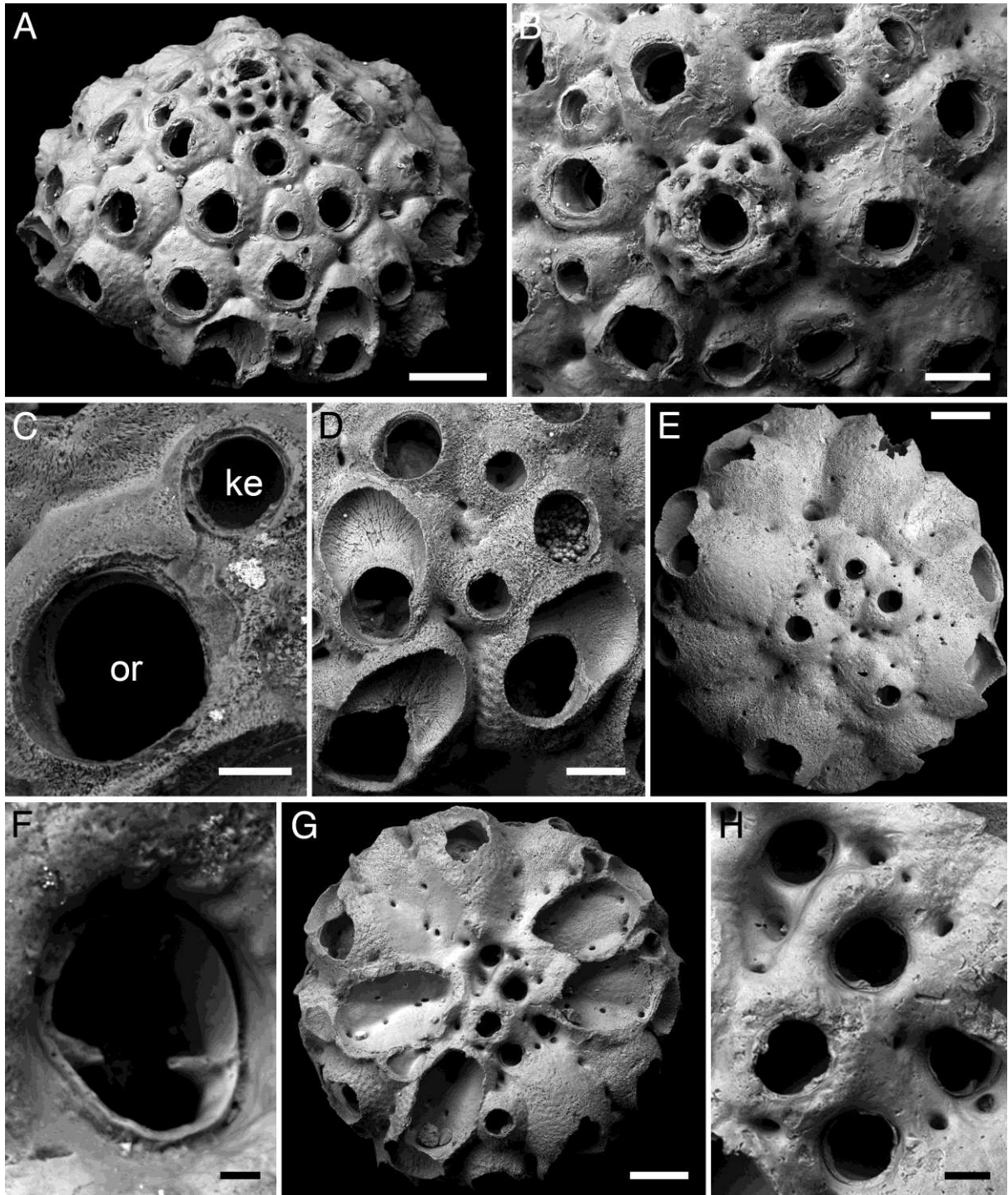
Figure 10. *Lacrimula crassa* sp. nov., Oligocene, Rupelian, TDP 17, Pande Peninsula, Kilwa District, Tanzania. **A, B,** holotype, NHMUK PI BZ 7800; **A,** general view of the colony; **B,** view of the adapical area from above. **C,** paratype, NHMUK PI BZ 7801, close-up of an

autozooidal orifice (or) in oblique view and a small polymorph interpreted as a kenozooid (ke). **D,** paratype, NHMUK PI BZ 7802, zooids of the proliferal region with reticulate frontal shield and ovicells with incomplete ooecia. **E, F,** paratype, NHMUK PI BZ 7803; **E,** view of the antapical surface of the colony with clustered polymorphs interpreted either as avicularia or kenozooids; **F,** close-up of a polymorph from the antapical region showing a distinct pair of condyles and interpreted as an avicularium. **G, H,** paratype, NHMUK PI BZ 7804, small polymorphs (either avicularia or kenozooids) at the antapical surface. Scale bars: A, E, G = 200 μm; B, D = 100 μm; C, H = 50 μm; F = 10 μm.

Supplemental material

Table 1. Data summary for TDP 17, Pande Peninsula, Kilwa District, Tanzania.